Mantle dynamics, post-perovskite and the role of pressure-dependent thermodynamic and transport properties

Nicola Tosi[1], Dave Yuen[2], Ondřej Čadek[3]

[1] Department of Planetary Physics, Institute of Planetary Research, DLR Berlin (Germany)

[2] Department of Geology and Geophysics, University of Minnesota, Minneapolis (USA)

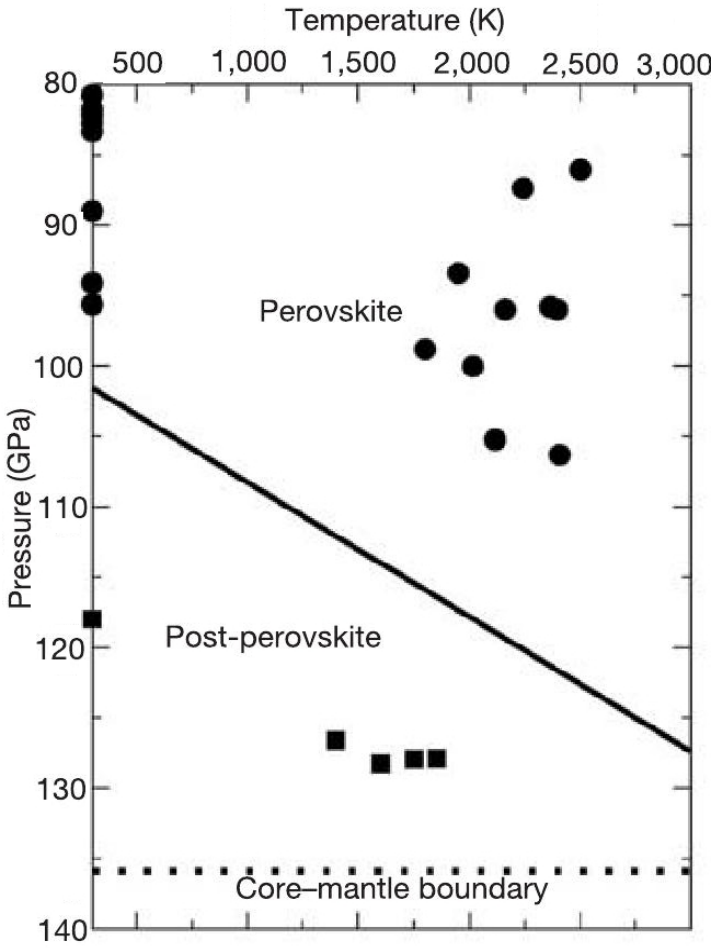
[3] Department of Geophysics, Charles University, Prague, (Czech Republic)

Deutsches Zentrum für Luft- und Raumfahrt e.V. in der Helmholtz-Gemeinschaft

Outline

- Post-perovskite and mantle dynamics
- Pressure dependence of thermal expansivity and conductivity
- Numerical model
- Dynamical consequences in the lower mantle ...
- ... and in the upper mantle
- Conclusions and perspectives

$MgSiO_3$ post-perovksite (ppv)



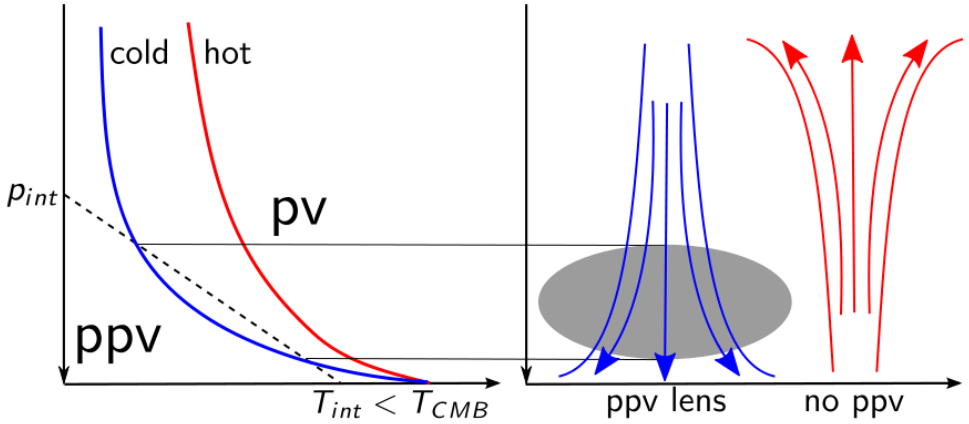
Oganov & Ono, *Nature* (2004)

- Deep exothermic phase change proposed to explain seismic discontinuities across the D'' layer (Sidorin et al., *Science*, 1999)
- 2004: Discovery of a new phase MgSiO3-pv → MgSiO3-ppv (Oganov & Ono, *Nature*, 2004; Murakami et al., *Science*, 2004)
- Pressure ~120 GPa (2700 km depth)
- Large positive Clapeyron slope 13.3 ± 1.0 MPa/K (Tateno et al., *EPSL*, 2009)
- Density increase ~1.5% (70 kg/m^3)

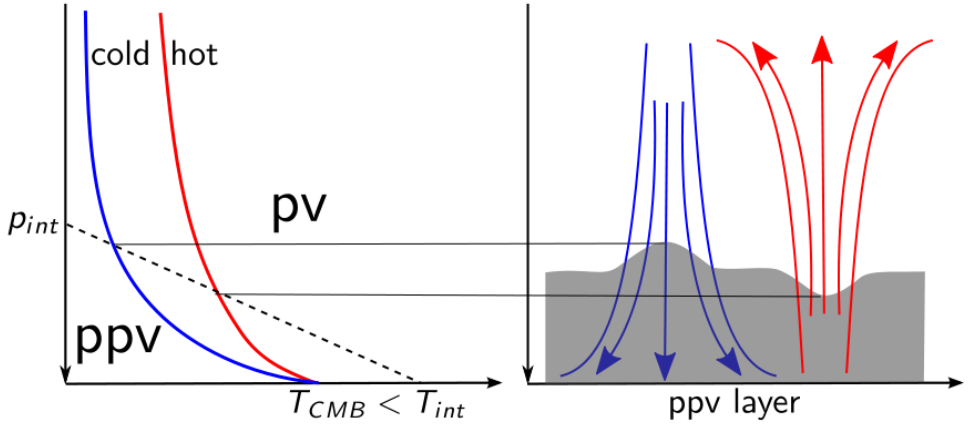
Crossing of the pv-ppv phase boundary

Single, double or no crossing according to the local geotherm and whether $T_{\text{int}} < T_{\text{CMB}}$ or $T_{\text{int}} > T_{\text{CMB}}$ (Hernlund et al., *Nature*, 2005)

Double crossing



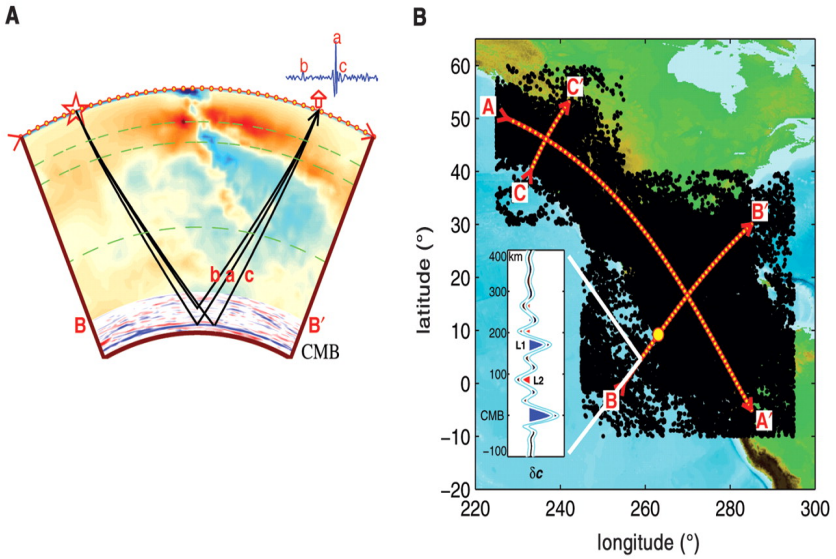
Single crossing



Seismic evidence for ppv

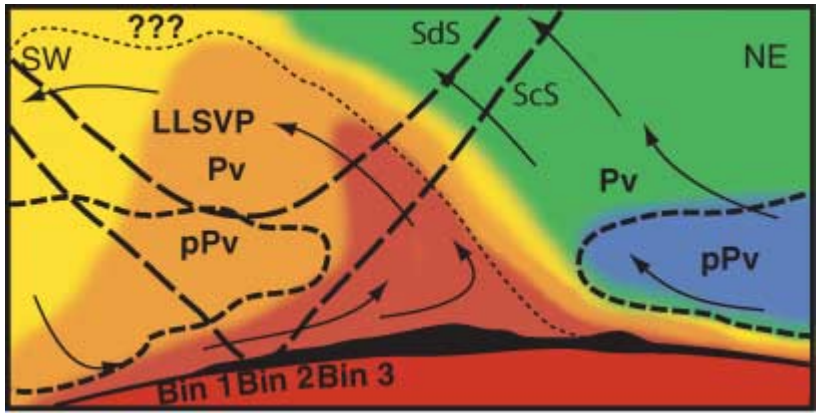
Observed discontinuities in shear-wave propagation near the CMB can be explained as the consequence of a pv-ppv phase change with double crossing, e.g.:

beneath Central America



van der Hilst et al., *Science* (2007)

beneath Central Pacific

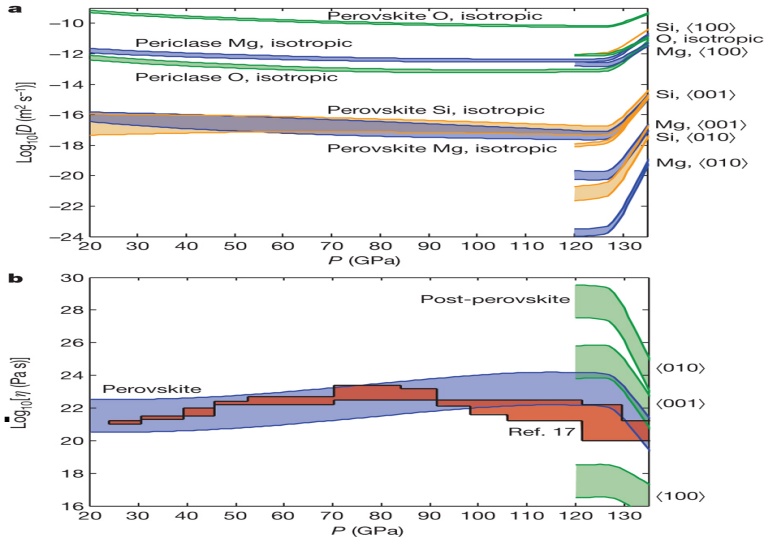


Lay et al., *Science* (2006)

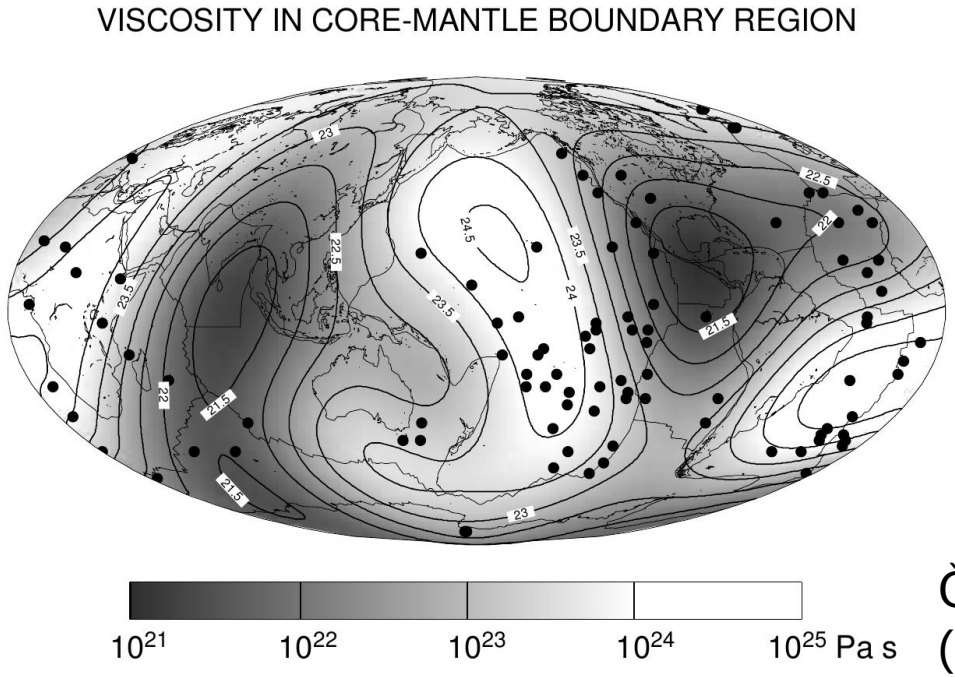
Rheology of ppv

- Still very uncertain (Karato, *PEPI*, 2010)
- Evidence for large anisotropy (Walte et al., *GRL*, 2009).
- Experimental evidence of weakening of $CaIrO_3$ during its transformation from pv to ppv by a factor 5-10 (Hunt et al., *Nat. Geosci.*, 2009).
- Fast diffusion rates for ppv with respect to pv from ab-initio simulations (Ammann et al., *Nature*, 2010).

Ammann et al. (2010)



Rheology of ppv

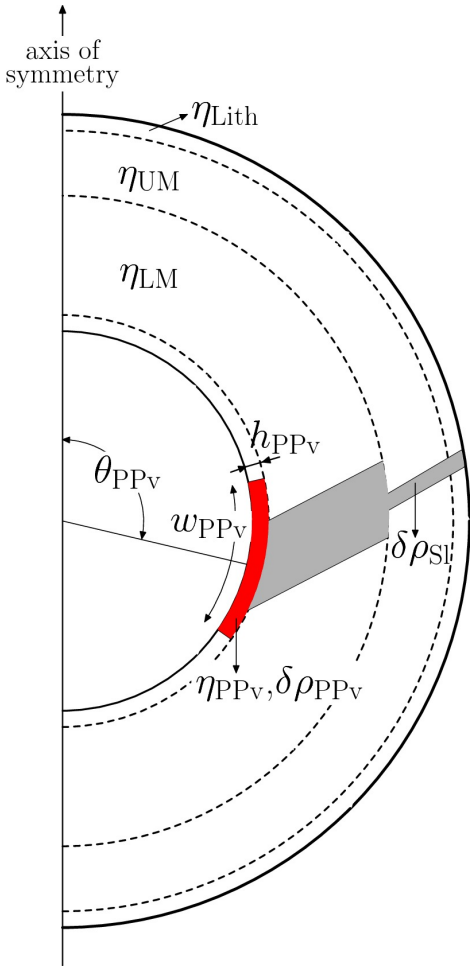


Čadek & Fleitout (2006)

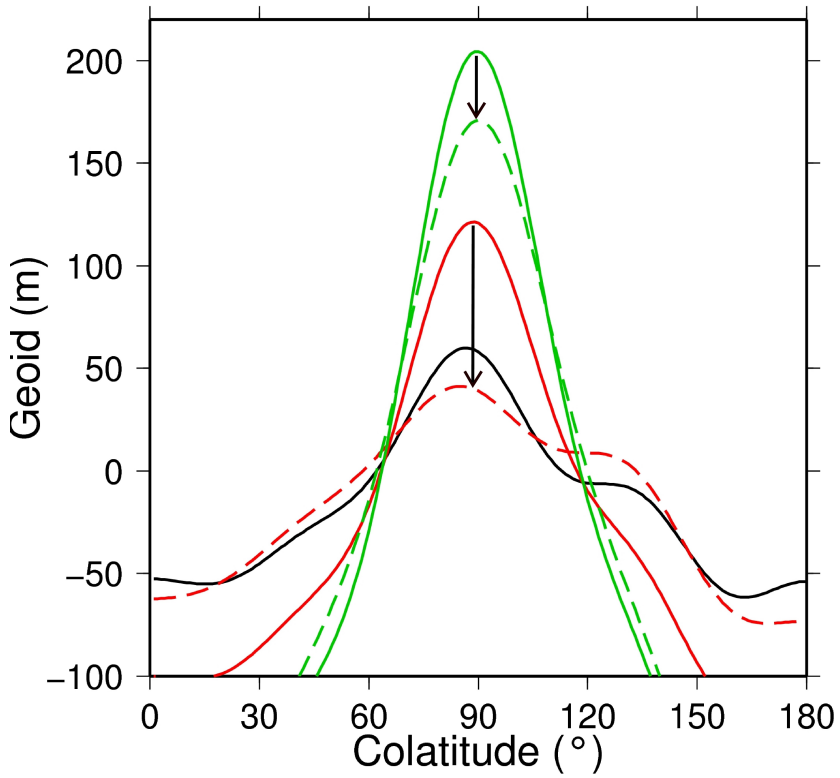
- Including lateral viscosity variations in D“ improves the fit to the geoid (Čadek & Fleitout, *SGG*, 2006).

- Significant correlation between low-viscosity areas and subduction sites

Low-viscosity ppv and subduction geoid



Tosi et al., *GRL*, 2009



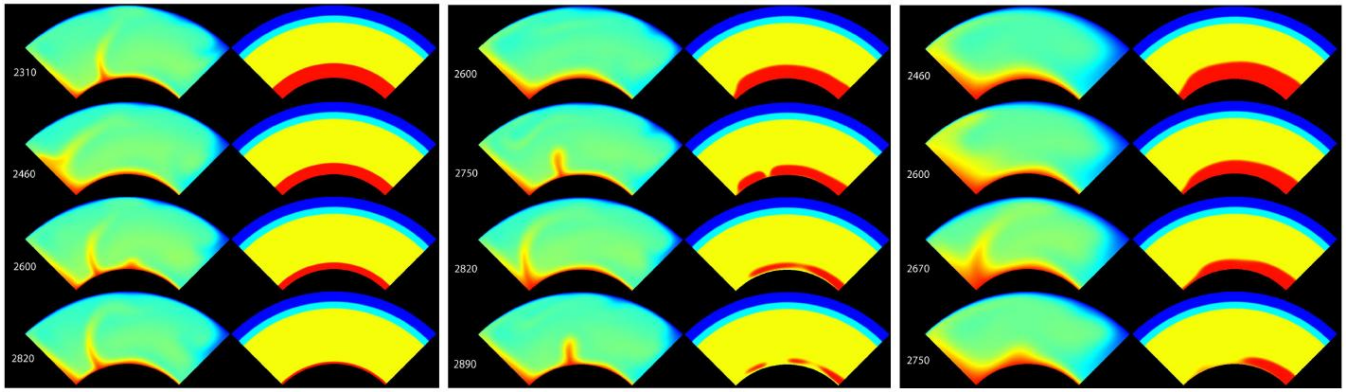
Radial viscosity: $\eta_{\mathrm{slab}}/\eta_{\mathrm{mantle}}=1$

Stiff slab: $\eta_{\mathrm{slab}}/\eta_{\mathrm{mantle}}=100$

Stiff slab: $\eta_{\mathrm{slab}}/\eta_{\mathrm{mantle}}=1000$

Mantle convection with ppv

- Small but measurable effects: slight increase of mantle temperature and efficiency of heat transport, increased instability of D'' (Nakagawa & Tackley, *GRL*, 2004).
- Reduced stability of thermochemical piles (Tackley et al., *AGU monograph*, 2007).
- Need for radiative thermal conductivity near the CMB to allow for the formation of long-wavelength structures (Matyska & Yuen, *EPSL*, 2006).
- Strong effetcts on the dynamics of D'' if ppv has low viscosity and small influence of dislocation creep (Čižková et al., *PEPI*, 2009).



Nakagawa & Tackley, *GRL* (2004)

Thermal expansivity

- Decrease of thermal expansivity with depth has long been recognized (Chopelas & Boehler, *GRL*, 1992)...
- …and included in mantle convection models (e.g. Hansen et al., *PEPI*, 1993).
- Recent high-pressure and high-temperature measurements of perovskite volume indicate a value of about 7 for the Anderson-Grüneisen parameter δ_T (Katsura et al., *GRL*, 2009):

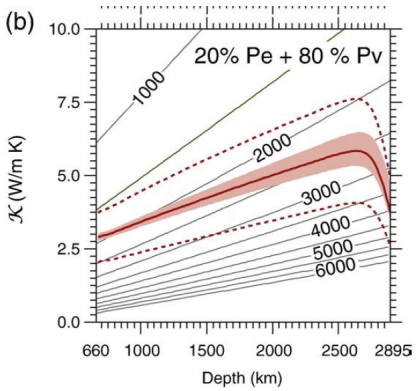
$$\frac{\alpha}{\alpha_0} = \left(\frac{\rho_0}{\rho} \right)^{\delta_T}$$

Thermal expansivity decreases by more than one order of magnitude throughout the mantle

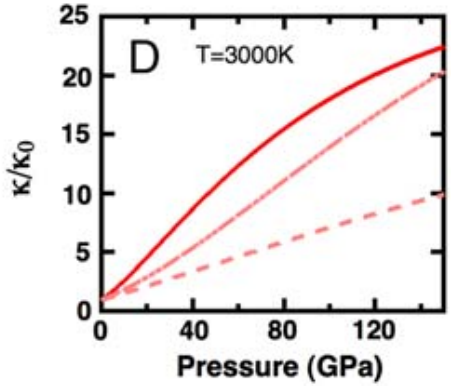
(Lattice) Thermal conductivity

- Several experiments and first-principle calculations have been conducted recently to determine the thermal conductivity of MgO and $MgSiO_3$ at lower mantle pressures. Assuming 20% MgO + 80% $MgSiO_3$:
  - k_{CMB} ~ 6 W/mK (de Koker, *EPSL*, 2010),
  - k_{CMB} ~ 10-15 W/mK (Goncharov et al., *PEPI*, 2009; Tang & Dong, *PNAS*, 2010; Ohta, *PhD*, 2010).
  - k_{CMB} ~ 20-30 W/mK (Hofmeister, *PEPI*, 2008).

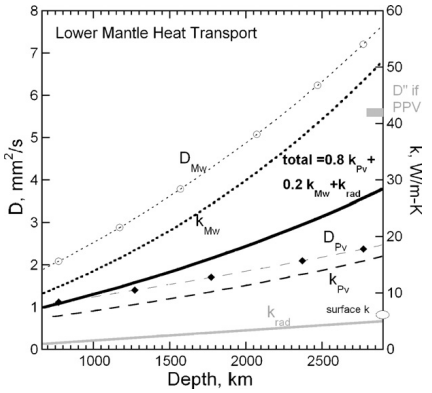
Thermal conductivity increases strongly with pressure



De Koker (2010)

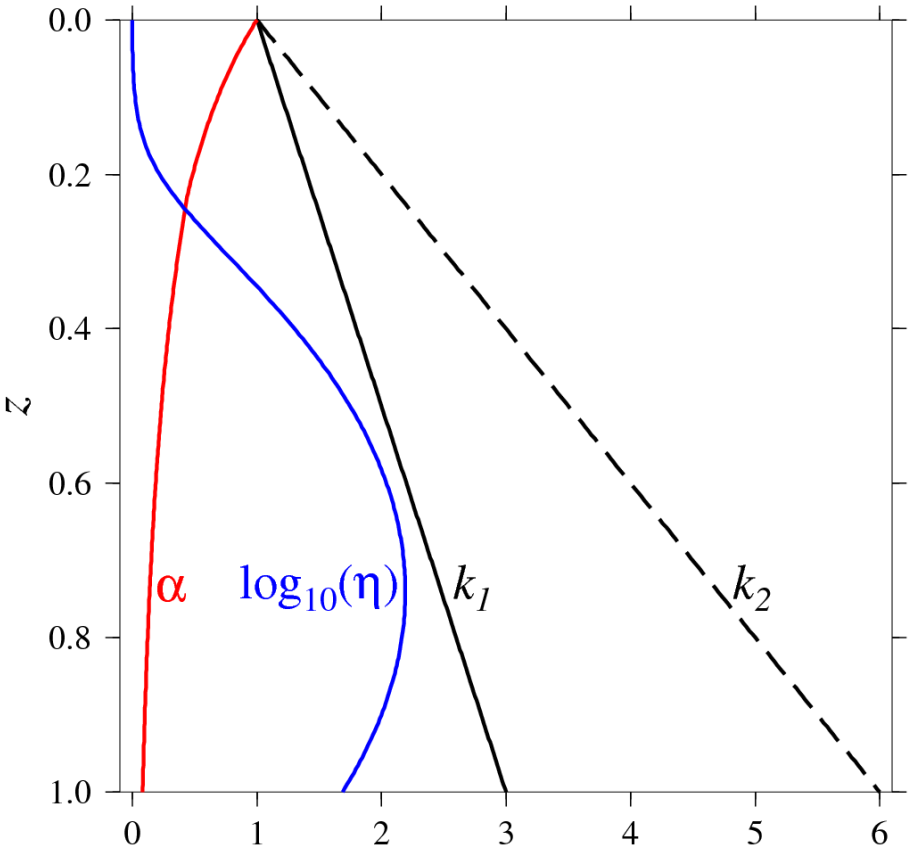


Tang & Dong (2010)



Hofmeister (2008)

Physical properties as a function of depth



Tosi et al., *EPSL* (2010)

- Thermal expansivity according to Katsura et al., *GRL* (2009).
- Linear increase of thermal conductivity such that k_{CMB}=10 W/mK (profile k_1) or k_{CMB}=20 W/mK (profile k_2).
- Depth-dependent part of viscosity derived from GIA inversion (Mitrovica & Forte, *EPSL*, 2004).

Model and equations

- 2D Cartesian box, aspect-ratio 10. Free-slip boundaries, isothermal top and bottom, reflecting sidewalls. Bottom heated. Temperature-, depth- and phase-dependent viscosity. Depth-dependent expansivity and conductivity.
- Extended Boussinesq Approximation:

Mass $$\nabla \cdot \vec{u} = 0$$

Momentum $$-\nabla p + \nabla \cdot \left(\eta \left(\nabla \vec{u} + (\nabla \vec{u})^t \right) \right) = \left(Ra_s (\alpha T - BC) + \sum_{i=1}^{3} Rb_i \Gamma_i \right) \vec{z}$$

Energy $$\frac{DT}{Dt} = \nabla \cdot (k \nabla T) + Di_s \alpha (T + T_0) u_z + \frac{Di_s}{Ra_s} \Phi + \sum_{i=1}^{3} \frac{Rb_i}{Ra_s} Di_s (T + T_0) \gamma_i \frac{D\Gamma_i}{Dt}$$

Composition $$\frac{DC}{Dt} = 0$$

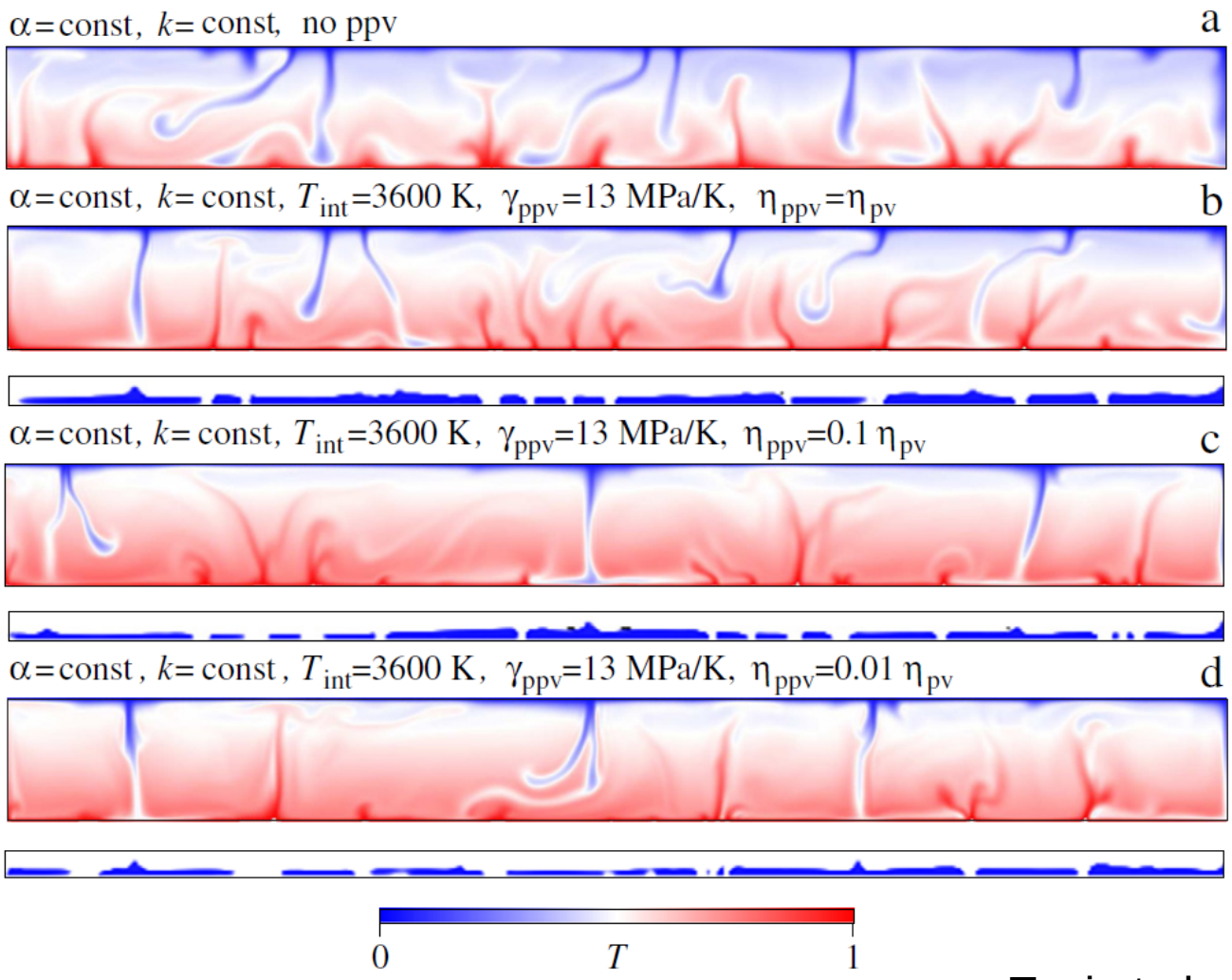
Numerical code

- **YACC** (Yet Another Convection Code):
  - primitive variables,
  - finite-volume,
  - semi-Lagrangian semi-implicit algorithm for advection-diffusion,
  - Lagrangian tracers for composition,
  - PARDISO - OpenMP direct solver,
  - extensively tested for Boussinesq and compressible convection (King et al., *GJI*, 2010) and thermo-chemical convection (van Keken et al., *JGR*, 1997; Schmeling et al., *PEPI*, 2008).
- Up to 1200 x 400 grid points with refinement near the boundary layers (~5 km vertical resolution near the CMB).

Parameters tested

- ppv viscosity: $\eta_{\mathrm{ppv}} = 1,\ 0.1,\ 0.01\,\eta_{\mathrm{pv}}$
- ppv phase parameters:
  - Temperature intercept: $T_{\mathrm{int}} = 3600,\ 4000\,\mathrm{K}\quad (T_{\mathrm{CMB}} = 3800\,\mathrm{K})$
  - Clapeyron slope: $\gamma_{\mathrm{ppv}} = 0,\ 9,\ 13\,\mathrm{MPa/K}$
- Depth-dependent thermal expansivity and conductivity
- Stability of a chemically distinct dense basal layer

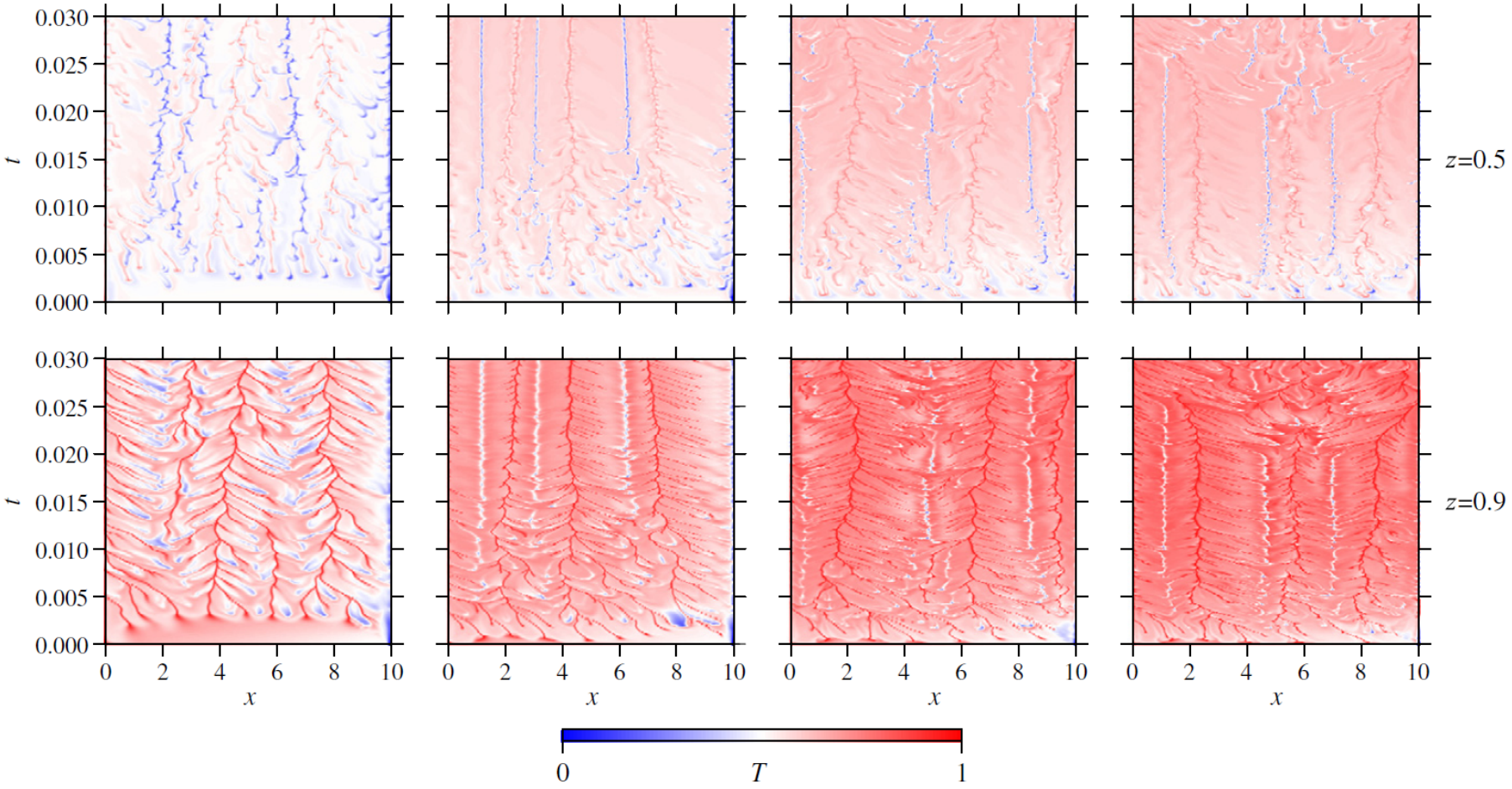
Effect of (low viscosity) ppv, α=const, k=const



Tosi et al., *EPSL* (2010)

Effect of (low viscosity) ppv, α=const, k=const

Time-history of the temperature at z=0.5 and z=0.9



Effect of (low viscosity) ppv, α=const, k=const

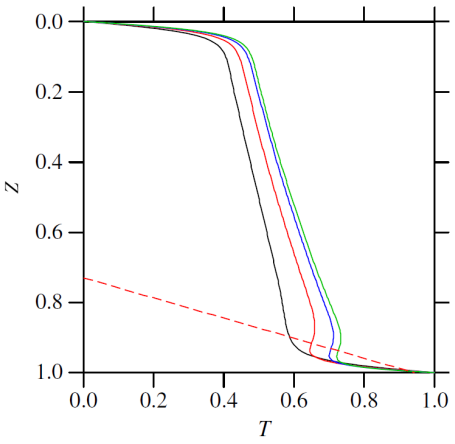
α = const, k=const, no ppv

α = const, k=const, T_{int} =3600 K, γ_{ppv} =13 MPa/K, $\eta_{ppv} = \eta_{pv}$

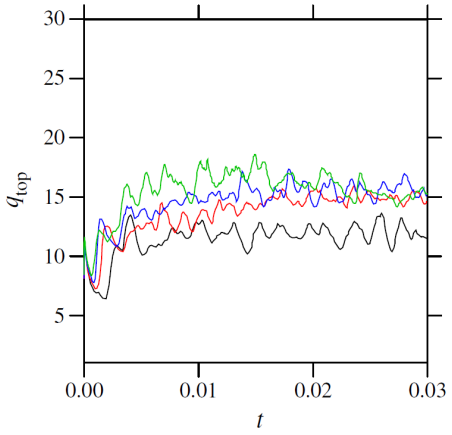
α = const, k=const, T_{int} =3600 K, γ_{ppv} =13 MPa/K, $\eta_{ppv} = 0.1\eta_{pv}$

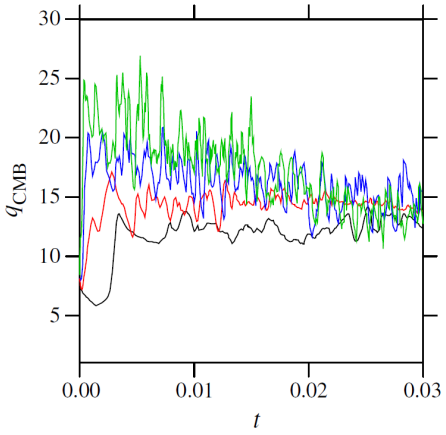
α = const, k=const, T_{int} =3600 K, γ_{ppv} =13 MPa/K, $\eta_{ppv} = 0.01\eta_{pv}$

Temperature

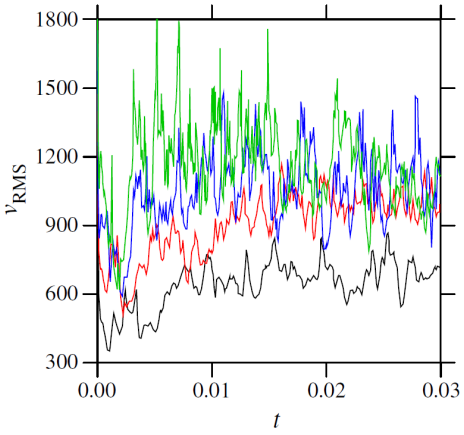


Heat fluxes





Flow



Systematic increase of mantle temperature, heat transport and time-dependence of the flow

Effect of ppv phase parameters (with $\eta_{ppv}=\eta_{pv}$)

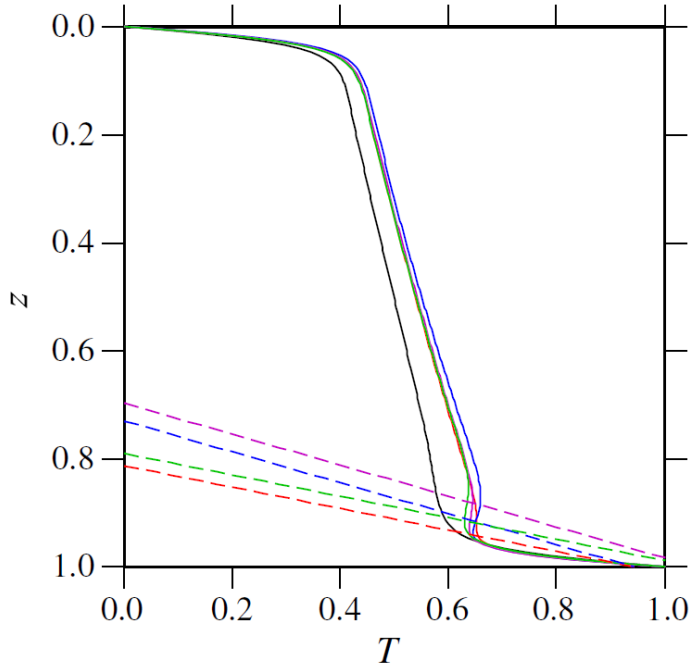
$\alpha = \text{const}$, $k = \text{const}$, no ppv

$\alpha = \text{const}$, $k = \text{const}$, $T_{int} = 3600$ K, $\gamma_{ppv} = 9$ MPa/K, $\eta_{ppv} = \eta_{pv}$

$\alpha = \text{const}$, $k = \text{const}$, $T_{int} = 3600$ K, $\gamma_{ppv} = 13$ MPa/K, $\eta_{ppv} = \eta_{pv}$

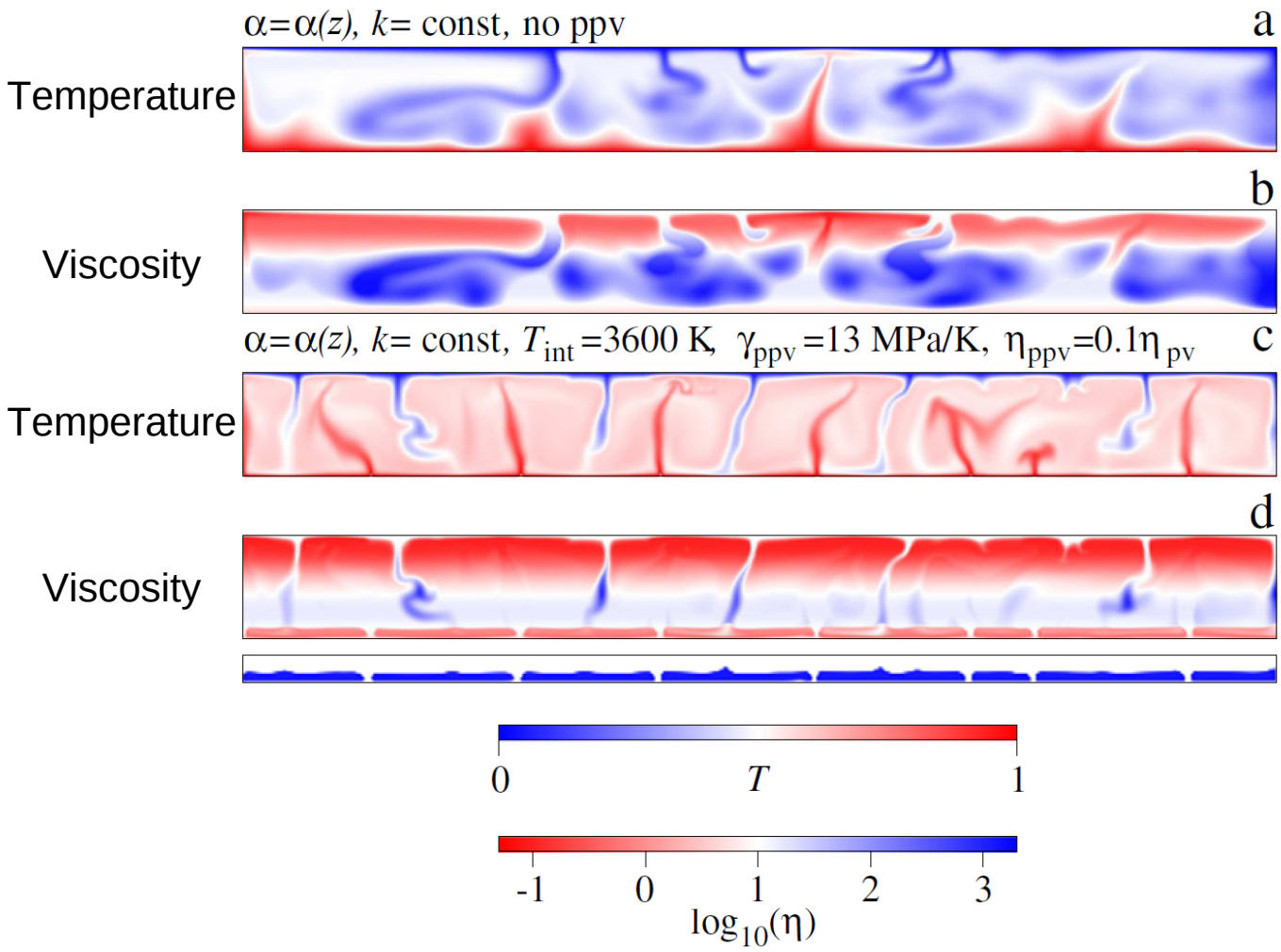
$\alpha = \text{const}$, $k = \text{const}$, $T_{int} = 4000$ K, $\gamma_{ppv} = 9$ MPa/K, $\eta_{ppv} = \eta_{pv}$

$\alpha = \text{const}$, $k = \text{const}$, $T_{int} = 4000$ K, $\gamma_{ppv} = 13$ MPa/K, $\eta_{ppv} = \eta_{pv}$



Small differences are observed using a smaller Clapeyron slope (γ_{ppv}=9 MPa/K) or a temperature intercept larger than the CMB temperature (T_{int}=4000 K).

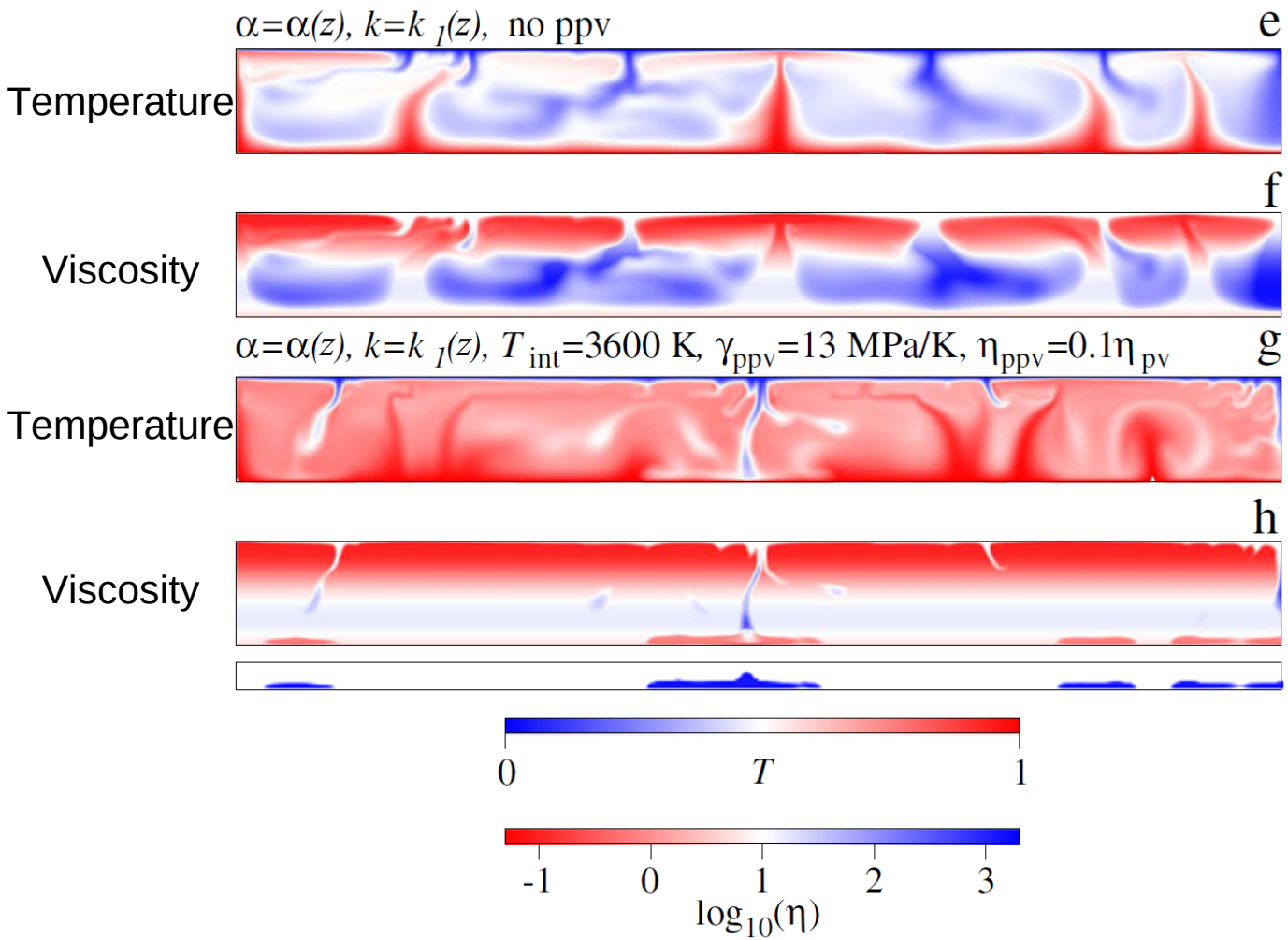
Effect of depth-dependent thermal expansivity (*k*=const)



With *α(z)* and no ppv, very sluggish regime, strong and large-sized plumes, cool mantle.

With *α(z)* and ppv, dramatic change in the dynamics of the system: hotter mantle because of more and stronger plumes.

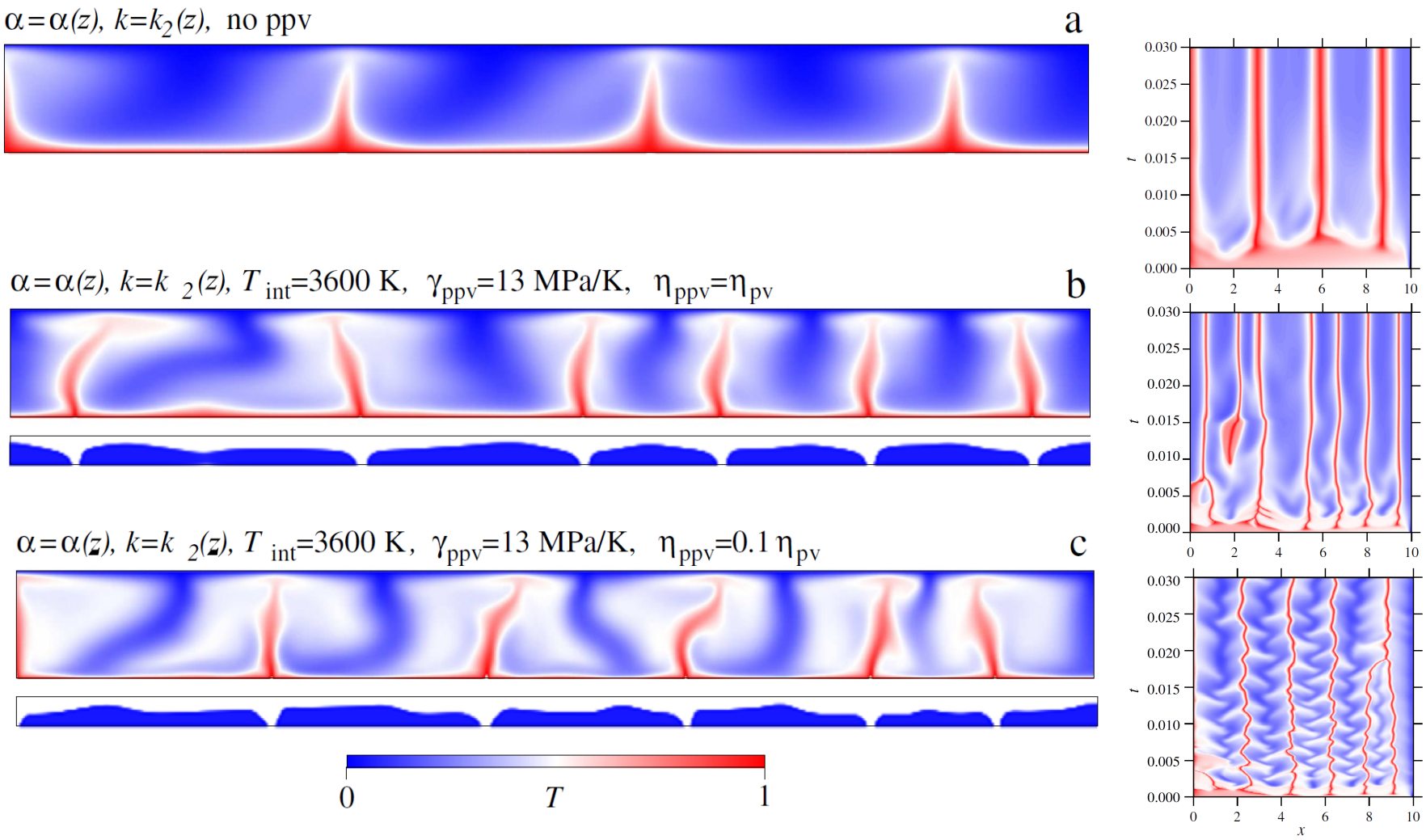
Combined effects of depth-dependent thermal expansivity and conductivity (k_{CMB}~10 W/mK)



With <u>α(z), k(z) and no ppv</u>, the dynamics is similar to cases in which *k*=const.

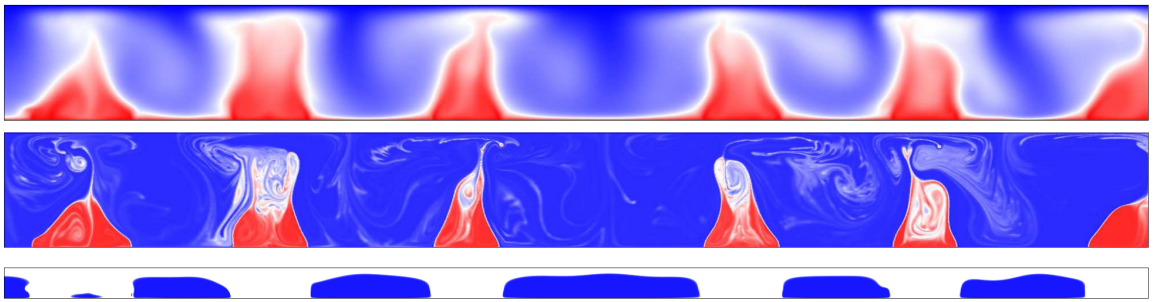
With <u>α(z), k(z) and ppv</u>, the effect of ppv is more pronounced: hotter mantle and large plumes clusters.

Combined effects of depth-dependent thermal expansivity and conductivity (k_{CMB}~20 W/mK)

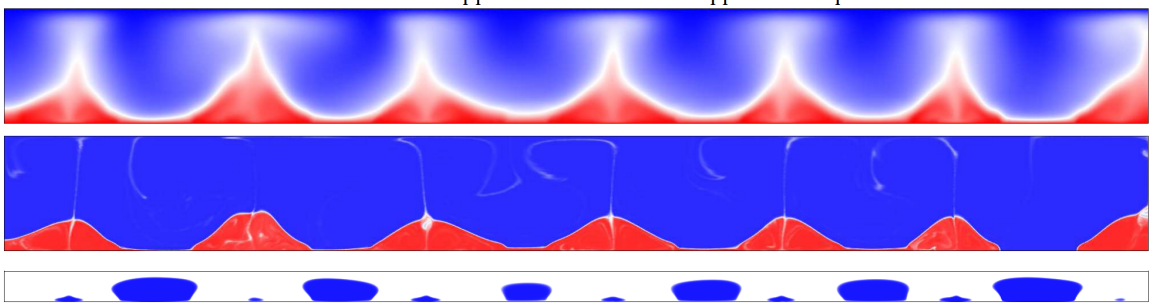


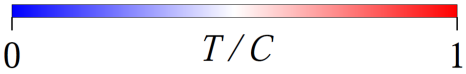
Stability of a dense basal layer (k_{CMB}~20 W/mK)

$\alpha=\alpha(z)$, $k=k_2(z)$, T_{int}=3600 K, γ_{ppv}=13 MPa/K, $\eta_{ppv}=0.1\eta_{pv}$, $\delta\rho$=2%



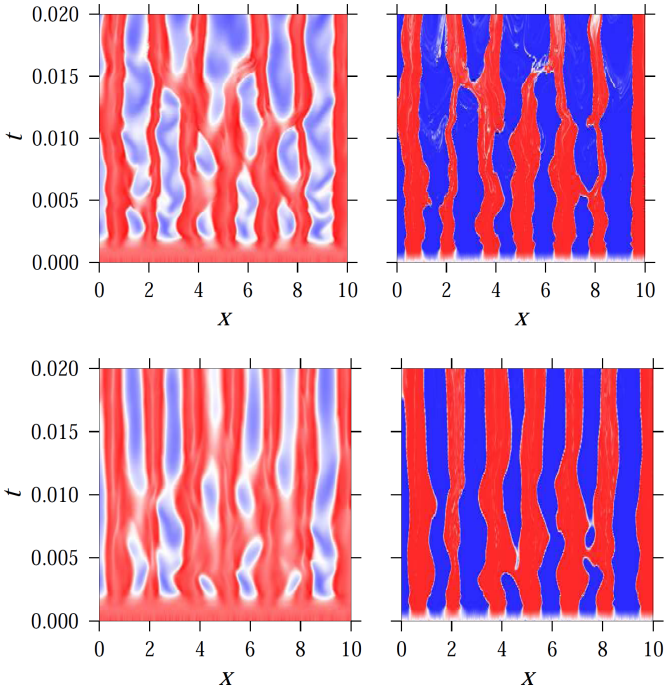
$\alpha=\alpha(z)$, $k=k_2(z)$, T_{int}=3600 K, γ_{ppv}=13 MPa/K, $\eta_{ppv}=0.1\eta_{pv}$, $\delta\rho$=4%





Time-history of

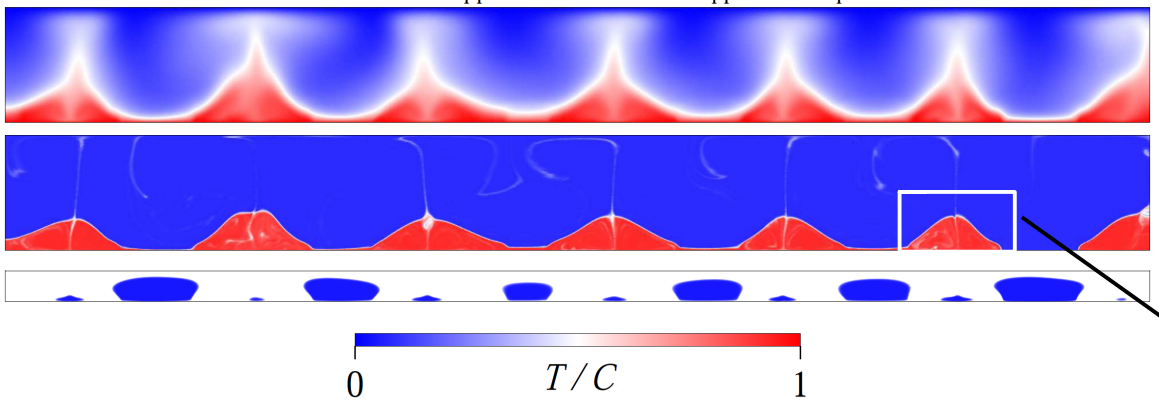
temperature composition



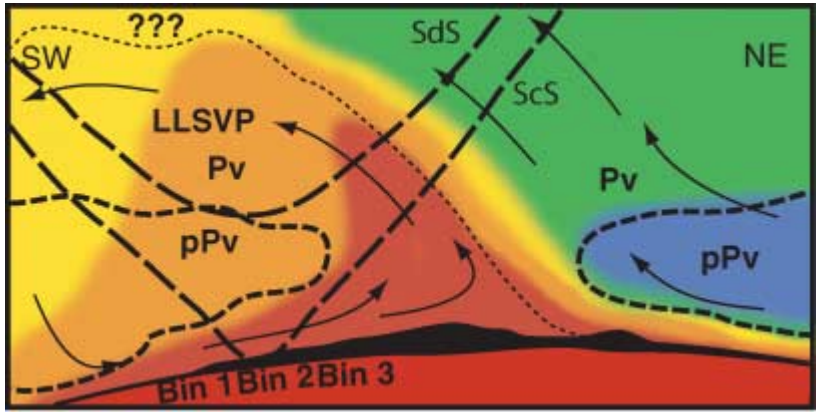
A large thermal conductivity in the deep mantle guarantees the long-term stability of large-scale thermo-chemical structures

Zoomed-in shot on a thermo-chemical pile

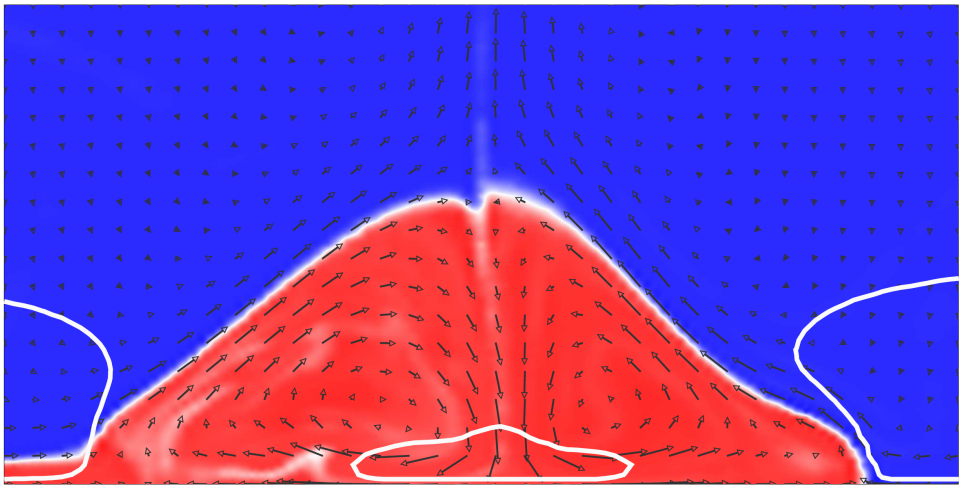
$\alpha=\alpha(z)$, $k=k_2(z)$, $T_{int}=3600$ K, $\gamma_{ppv}=13$ MPa/K, $\eta_{ppv}=0.1\eta_{pv}$, $\delta\rho=4\%$



ppv is obtained due to secondary circulation within the termo-chemical pile

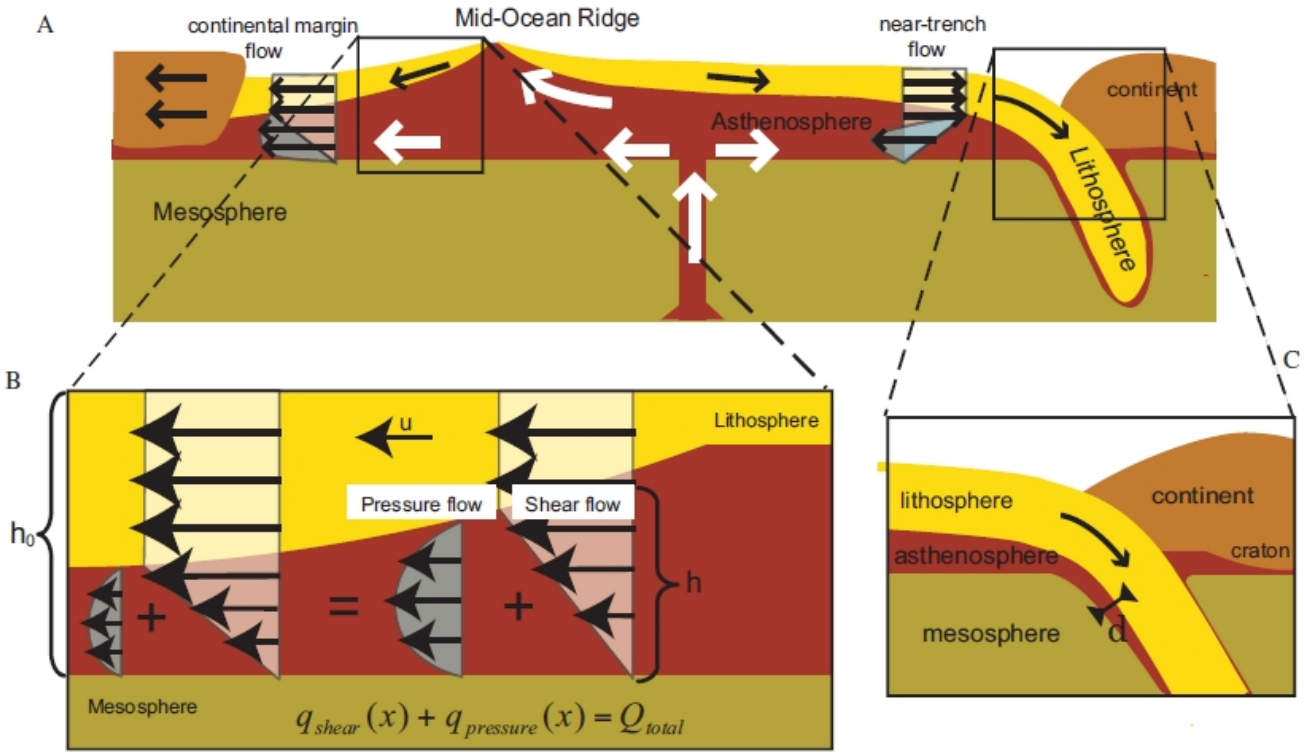


Lay et al., *Science* (2006)



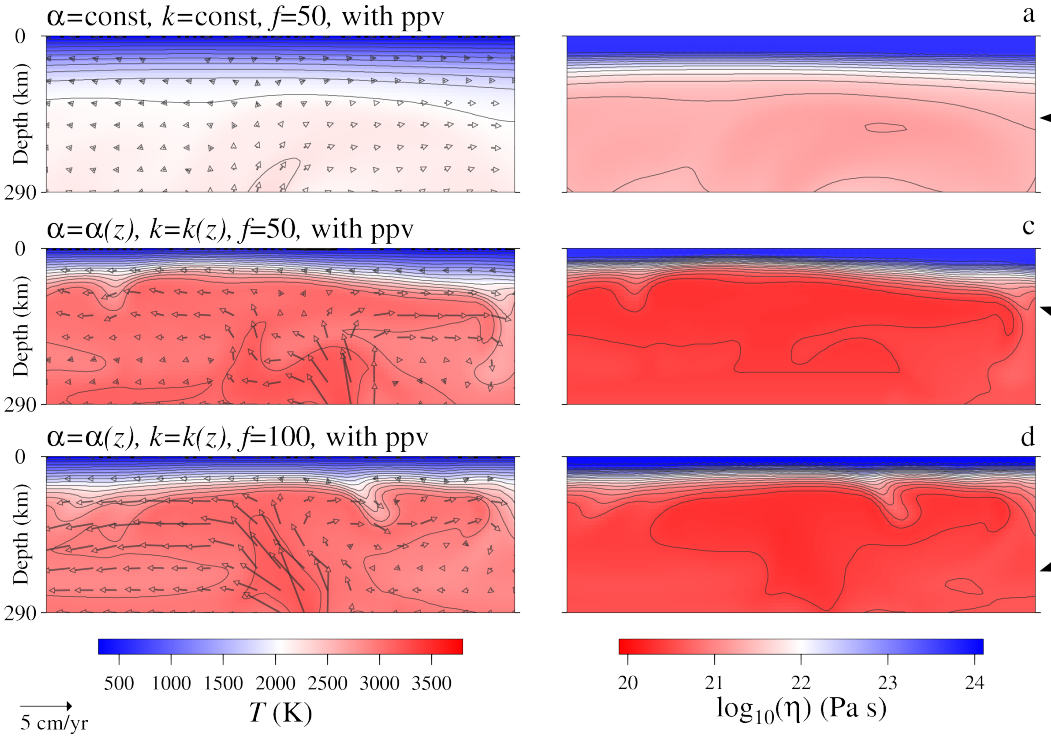
Plume-fed asthenosphere

Do lower mantle properties play a role in the formation of a regional, low-viscosity asthenosphere?



Yamamoto et al., *GSA*, 2007.

Lower mantle properties and asthenosphere (with ppv)

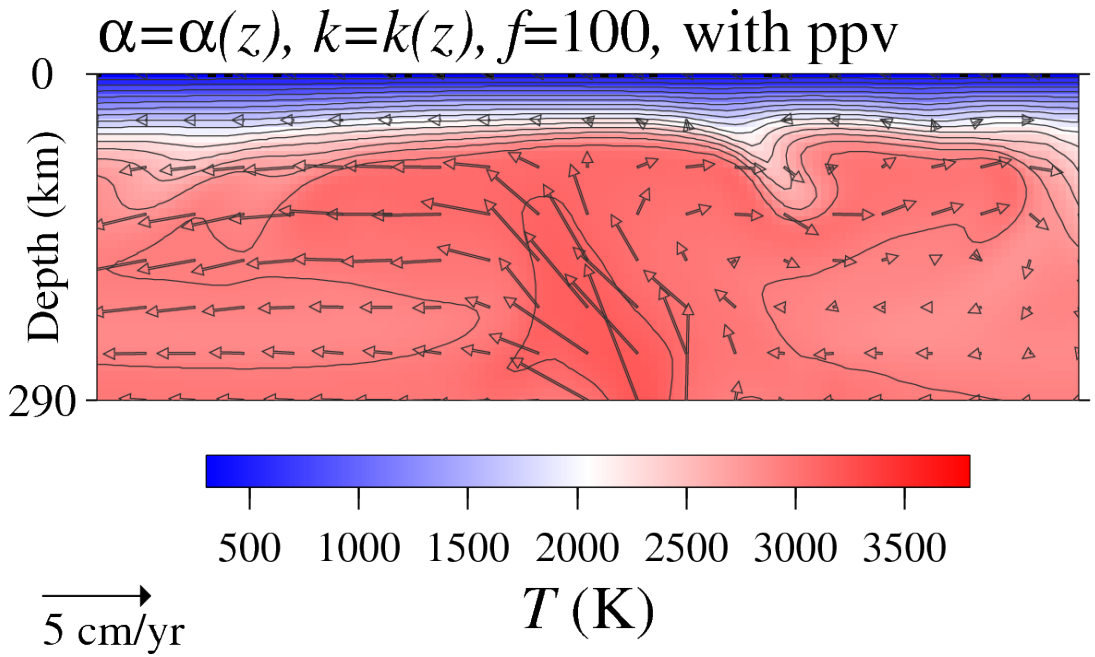


Models with constant conductivity and expansivity (a) do not deliver strong enough plumes.

Models with depth-dependent conductivity and expansivity (b-d) facilitate the formation of a regional low-viscosity asthenosphere.

Lower mantle properties and asthenosphere

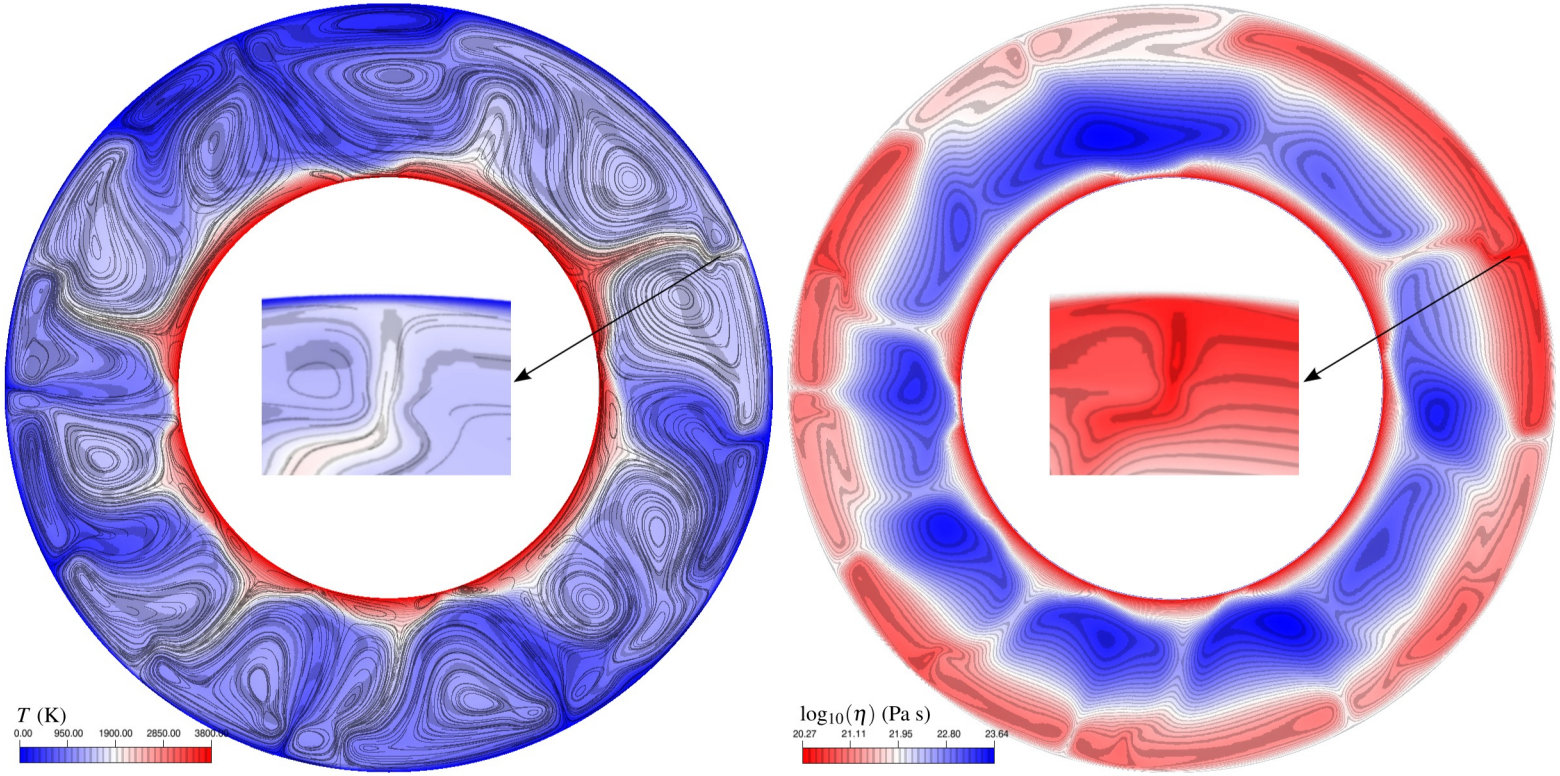
Problem: Cartesian models produce very high temperatures that would lead to large-scale melting in the upper-mantle above 400 km depth



Lower mantle properties and asthenosphere

Under the same conditions, cylindrical models exhibit upper mantle temperatures up to 500 K cooler, while the basic dynamics remains unaltered

$\alpha = \alpha(z)$, $k = k(z)$, f =50, with ppv



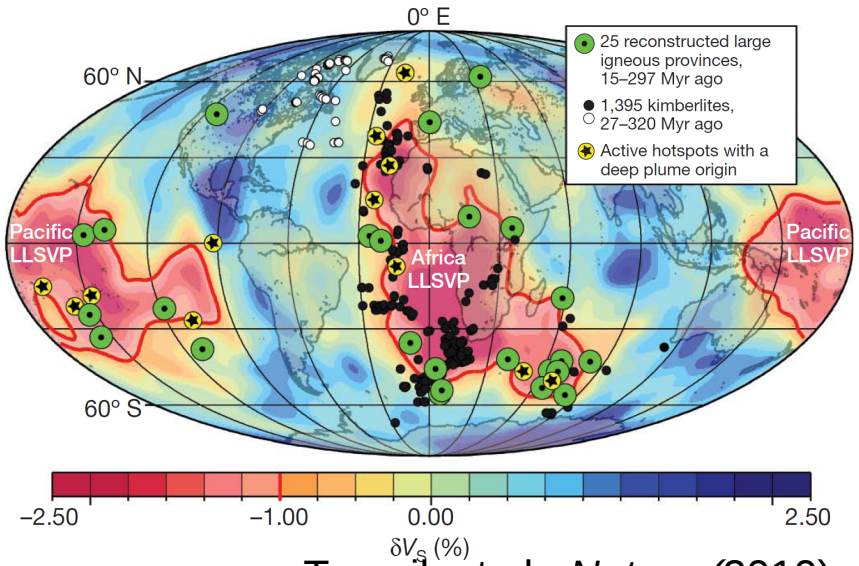
Conclusions

- With constant expansivity and conductivity, the effect of ppv is small but measurable: **hotter geotherm, higher heat fluxes, shorter-scale instabilities near CMB**.
- The choice of different phase parameters for ppv (Clapeyron slope and temperature intercept at CMB) **does not play a significant role**.
- The combination of depth-dependent viscosity, expansivity and conductivity causes a **sluggish regime with large-sized upwellings**. Downgoing **slabs loose their buoyancy and stagnate in the mid mantle** causing a **cold geotherm**.
- With depth-dependent expansivity and conductivity, the effect of ppv becomes a **first-order feature: much hotter mantle due to large and vigorous upwellings**.
- Upper mantle temperatures become too large. A cylindrical geometry allows us to restore more realistic temperatures while leaving the basic dynamics unaltered.

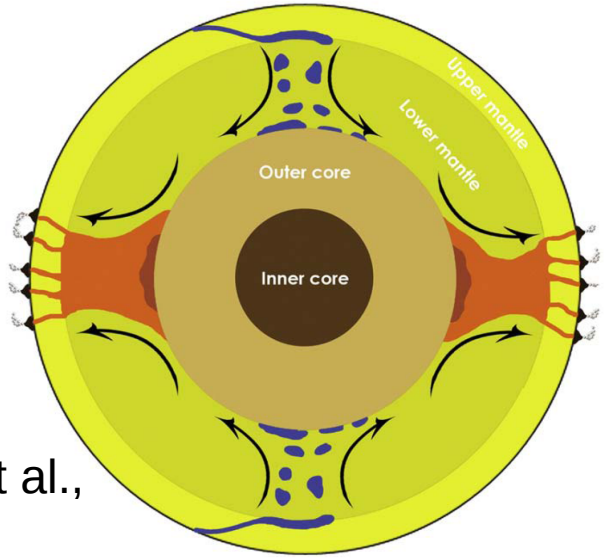
Conclusions

- With k_{CMB}~20 W/mK, a **quasi steady-state regime** is obtained, even in the presence of low viscosity ppv, for both thermal and thermo-chemical models (Torsvik et al., *Nature*, 2010). "Bottom-up" dynamics with a prominent role for large-scale plumes (Dziewonski et al., *EPSL*, 2010).

- Effect of spherical geometry, role of internal heating and plate-like rheology have yet to be explored.



Torsvik et al., *Nature* (2010)



Dziewonski et al., *EPSL* (2010)